Special Collection

An Experimental Toolbox for Structure-Based Hit Discovery for *P. aeruginosa* FabF, a Promising Target for Antibiotics

Ludvik Olai Espeland+,[a, b] Charis Georgiou+,[a] Raphael Klein+,[a, c] Hemalatha Bhukya,[d] Bengt Erik Haug,[b] Jarl Underhaug,[b] Prathama S. Mainkar,[d] and Ruth Brenk*[a]

FabF (3-oxoacyl-[acyl-carrier-protein] synthase 2), which catalyses the rate limiting condensation reaction in the fatty acid synthesis II pathway, is an attractive target for new antibiotics. Here, we focus on FabF from *P. aeruginosa* (*Pa*FabF) as antibiotics against this pathogen are urgently needed. To facilitate exploration of this target we have set up an experimental toolbox consisting of binding assays using bio-layer interferometry (BLI) as well as saturation transfer difference (STD) and WaterLOGSY NMR in addition to robust conditions for structure determination. The suitability of the toolbox to support structure-based design of FabF inhibitors was demonstrated through the validation of hits obtained from virtual screening. Screening a library of almost 5 million compounds resulted in 6 compounds for which binding into the malonyl-binding site of FabF was shown. For one of the hits, the crystal structure in complex with *Pa*FabF was determined. Based on the obtained binding mode, analogues were designed and synthesised, but affinity could not be improved. This work has laid the foundation for structure-based exploration of *Pa*FabF.

Introduction

New antibiotics are urgently needed to maintain the high standard of living that we have got accustomed to.[1] In response to this, the World Health Organization has recently published a list of bacteria for which antibiotics are in high demand and urged that research and drug discovery efforts are directed toward these bacteria.[2] However, most of the compounds in clinical development are not fit for purpose as they are derivatives of already known antibiotics and therefore have cross-resistance with existing agents. Accordingly, there is a high need for new classes of antibiotics without pre-existing cross-resistance. To achieve this, we need more knowledge on new targets and new chemical scaffolds.[3]

[a] L. O. Espeland,+ Dr. C. Georgiou,+ Dr. R. Klein,+ Prof. Dr. R. Brenk
     Department of Biomedicine, University of Bergen
     Jonas Lies Vei 91, 5020 Bergen (Norway)
     E-mail: ruth.brenk@uib.no
[b] L. O. Espeland,+ Prof. Dr. B. E. Haug, Assoc. Prof. Dr. J. Underhaug
     Department of Chemistry, University of Bergen
     Allégaten 41, 5007 Bergen (Norway)
[c]   Dr. R. Klein+
     Institute of Pharmacy and Biochemistry
     Johannes Gutenberg University
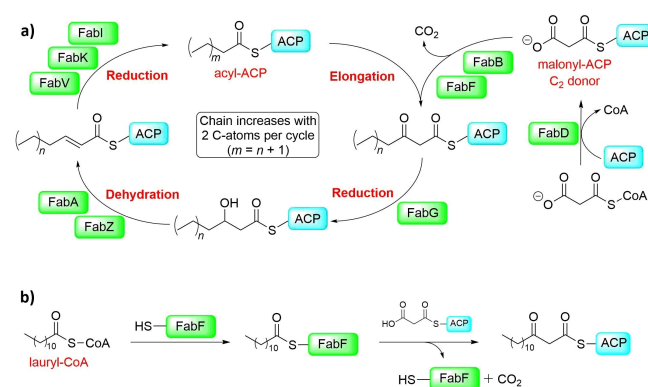   Staudingerweg 5, 55128 Mainz (Germany)
[d] H. Bhukya, Dr. P. S. Mainkar
     Department of Organic Synthesis & Process Chemistry
     CSIR-Indian Institute of Chemical Technology
     Tarnaka, Hyderabad 500007 (India)

[+] These authors contributed equally to this work.

💻 Supporting information for this article is available on the WWW under https://doi.org/10.1002/cmdc.202100302

Special Collection This article belongs to the Special Collection "Nordic Medicinal Chemistry".

A possible source for new targets for antibiotics is the fatty acid synthesis (FAS II) pathway (Figure 1a).[4] In this pathway, fatty acid synthesis is carried out by a series of monofunctional enzymes which are highly conserved among microbial pathogens. In contrast, mammals use the FAS I pathway consisting of the large multifunctional enzyme fatty acid synthase.[5] The fatty acid synthase and the enzymes of the FAS II pathway differ significantly enabling the development of selective inhibitors. While the FAS II pathway is also present in mitochondria of human cells, its role is not entirely clear, and short-term inhibition by antibiotics is likely to be tolerated.[6] Genes coding for enzymes in the FAS II pathway have been found to be essential in several genetic screens.[7–11] Further validation of this pathway as a target for antibiotics comes from the drug isoniazid which is in clinical use against tuberculosis. The main target for isoniazid is the enoyl-ACP reductase FabI, which is part of the FAS II pathway (Figure 1a).[4] Multiple enzymes in

Figure 1. Fatty acid synthesis in bacteria. a) Schematic overview of the elongation part of the FAS II pathway. b) Condensation reaction catalysed by FabF. (ACP: acyl carrier protein).

ChemMedChem

Full Papers
doi.org/10.1002/cmdc.202100302

Chemistry
Europe
European Chemical
Societies Publishing

this pathway were predicted to contain druggable binding sites rendering them attractive targets for antibiotic drug discovery.[12]

Here, we focus on 3-oxoacyl-[acyl-carrier-protein] synthase 2 (also called beta-ketoacyl-ACP synthase 2 with FabF, Kas II, and KasB as commonly used short names). FabF catalyses the rate limiting condensation of malonyl-ACP (acyl carrier protein) with acyl-ACP (Figure 1b),[4] facilitated by the catalytic Cys-His-His triad. FabB catalyses the same reaction (Figure 1a) but differs in substrate specificity for the fatty acid chain. FabF has been validated in Gram-positive bacteria as the target for the natural products platensimycin, platencin and fasamycin A and B (Figure 2).[13–15] Platensimycin, although inactive against wild-type Gram-negative bacteria, is active against efflux-negative *E. coli.*[13] Similarly, the fasamycins are active against membrane-permeabilized *E. coli* but not the unaltered strain.[14] These observations suggest that the lack of activity of these compounds against Gram-negative bacteria is not caused by a lack of essentiality of the target but owing to the inability of the ligands to access it. Further target validation for FabF comes from the natural products cerulenin and thiolactomycin (Figure 2). Cerulenin is a covalent inhibitor forming a bond with the catalytic cysteine.[16–18] Both natural products are effective against bacteria and thiolactomycin is also efficacious in an animal model, however both lack selectivity and potency for clinical use.[4]

The crystal structures of FabF and the related FabB from various bacteria have been determined revealing the architecture of the binding site. The active site contains two sub-pockets: one for accommodating the growing fatty acid chain and one for binding the C_2-donor malonyl-ACP. The inhibitors platensimycin, platencin, and thiolactomycin all bind into the malonyl-ACP pocket whereas cerulenin binds into the fatty acid channel.[13,19–21] However, platensimycin and platencin do not bind strongly to the w.t. enzyme, but only to the lauroyl-FabF intermediate (Figure 1b) and to intermediate-mimicking FabF variants in which the active site Cys has been changed to either Gln or Ala.[13,19] The lack of binding to the w.t. enzyme is probably caused by repulsion between the carboxylate group of these compounds and the active site nucleophilic Cys residue (Figure 3). The benzoic acid moiety of platensimycin is deeply
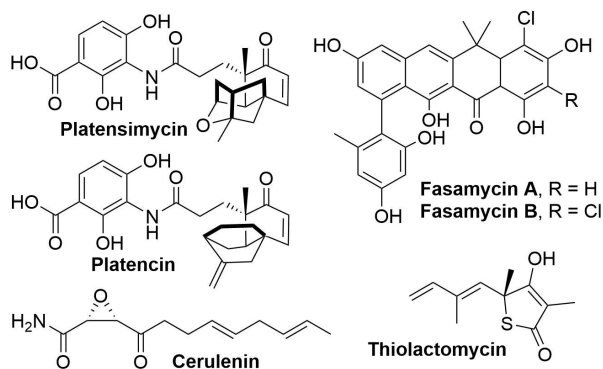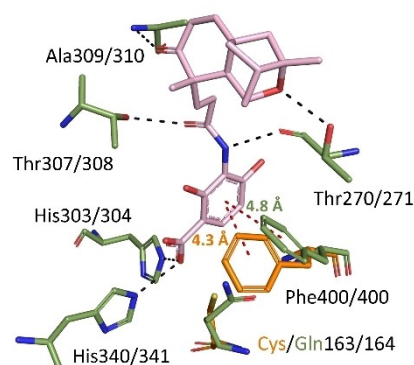

Figure 3. Alignment of apo w.t. *Ec*FabF (orange sticks – PDB ID: 2GFW, for clarity only Phe400 is shown) and *Ec*FabF C163Q (green sticks – PDB ID: 2GFX) in complex with platensimycin (pink sticks). Hydrogen bonds are indicated as black dashed lines and aromatic interactions as red dashed lines. For easier comparison to *Pa*FabF all residues are labelled as *Ec*FabF/*Pa*FabF. Compared to the apo structure, Phe400 is rotated in the holo structure to create space for the ligand to bind.

bound in the malonyl pocket and forms hydrogen bonds with the catalytic histidines and edge-face interactions with Phe400/400 (*E. coli* FabF (*Ec*FabF)/*P. aeruginosa* FabF (*Pa*FabF) numbering). The rather hydrophobic aliphatic ring system extends towards the opening of the pockets and is held in place by hydrogen bonds with Thr270/271 and Ala309/310. In addition, the amide linker forms hydrogen bonds to Thr307/308.

Platensimycin is the most potent FabF inhibitor known to date. Using the radioactively labelled compound in displacement assays, it was determined that platensimycin binds with an IC_{50} of 19 nM to the lauroyl-FabF intermediate while binding to the w.t. enzyme is much weaker.[13] Total synthesis of platencin[22,23] and platensimycin[24,25] have been carried out, and efforts have been undertaken to increase the antibiotic activity through synthesis of analogues. For platensimycin, this includes the modifications of the benzoic acid head group[26,27] and the tetracyclic cage.[28–32] While some of these compounds showed promising activity against Gram-positive bacteria, for most compounds activity against Gram-negative bacteria was not reported. In addition, poor pharmacokinetic properties were also a concern.

To further assess FabF as a target, there is a need for more readily modifiable ligands, ideally also based on diverse scaffolds. Only limited efforts towards obtaining such compounds have been published. Using the crystal structure of *Ec*FabB, Zheng et al. have conducted a virtual screening which resulted in the identification of a series of benzoxazolinones where the most potent compound had an IC_{50} of 235 μM against *Ec*FabB and 387 μM against *S. aureus* FabF.[33] Further, N-acetylated sulfonamides have been reported as the result of a phenotypic screen and found to be highly specific for *C. trachomatis* FabF, albeit their binding modes remain elusive.[33]

Here, we report on our efforts toward establishing an experimental toolbox for structure-based drug design for FabF from *P. aeruginosa* to drive forward the exploration of FabF as a

Figure 2. Natural product FabF inhibitors.

ChemMedChem

Full Papers
doi.org/10.1002/cmdc.202100302

Chemistry Europe
European Chemical
Societies Publishing

drug target for Gram-negative bacteria. The target organism was chosen as there is a particular high need for new antibiotics to fight infections caused by carbapenem-resistant *P. aeruginosa*.[2] Starting from our previous structural experience with *Pa*FabF[34] we have established robust crystallization conditions that allow for soaking with ligands. Further, we have developed a binding assay using bio-layer interferometry (BLI). In addition, we have set up saturation transfer difference (STD) and WaterLOGSY NMR assays for binding and competition experiments to confirm active site binding. We demonstrate the suitability of this toolbox for structure-based ligand discovery through the validation of hits obtained from virtual screening.

Results and Discussion

As *Pa*FabF is a promising target for new antibiotics, we aimed at establishing an experimental toolbox that would enable the structure-based design of new ligands. This toolbox should contain binding assays as well as robust conditions for soaking crystals to allow for a thorough assessment of potential ligands.

*Pa*FabF binding assay based on BLI

In order to determine ligand binding to *Pa*FabF and the intermediate-mimicking FabF variants C164Q and C164A, a BLI assay was developed. For this purpose, protein constructs containing an AviTag[35] that can be enzymatically biotinylated using the biotin ligase BirA[36] were designed and purified as described earlier.[34] Avi-tagged *Pa*FabF C164Q was prone to precipitation and thus not accessible for BLI experiments. Therefore, *Pa*FabF C164Q without an Avi-tag was chemically biotinylated using NHS-PEG$_4$-biotin. The biotinylated *Pa*FabF variants were immobilized on Super Streptavidin (SSA) biosensors. Binding of ligands at different concentrations was recorded as wavelength shift of the interference pattern of white light reflected from a layer of immobilized protein on the biosensor tip, and an internal reference layer.[37] At concentrations up to 5 and 50 μM respectively, no binding for platensimycin and platencin to the w.t. enzyme was observed. In contrast, binding constants of 0.52 and 2.75 μM, respectively were determined for *Pa*FabF C164A (Figure 4 and Figure S8 in Supporting Information). Using chemically biotinylated *Pa*FabF C164Q, a similar binding constant for platencin was determined (2.30 μM, data not shown). As the C164A variant was more stable under assay conditions, this protein was mainly used for subsequent binding assays.

The binding data obtained from the BLI assay is overall in agreement with what has been reported previously for these ligands when measured against *Ec*FabF. In an assay based on displacement of a radioactive platensimycin derivative from the lauroyl-*Ec*FabF intermediate, IC$_{50}$ values of 19 nM and 113 nM were reported for platensimycin and platencin, respectively.[13,15] Using the same assay, no IC$_{50}$ values could be determined for platensimycin binding to w.t. *Ec*FabF.[13] While the binding constants for platensimycin and platencin binding to *Pa*FabF
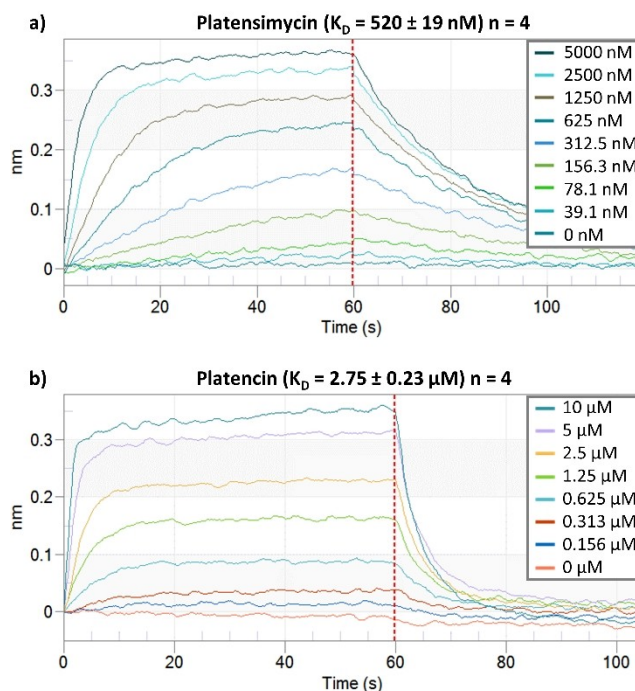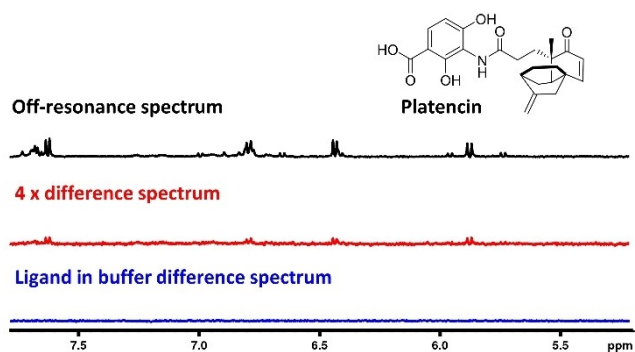

Figure 4. BLI sensorgram for a) platensimycin and b) platencin binding to PaFabF C164A. The dashed red line indicates the start of the dissociation interval.

C164A were higher than those for the *Ec*FabF construct, in both cases they differed about 5-fold. Using an enzymatic elongation assay with *Ec*FabF, the IC$_{50}$ values for platensimycin and platencin were determined as 0.29 and 4.9 μM, respectively.[15] The latter values are close to the K$_D$ values for *Pa*FabF C164A obtained using BLI.

NMR assay to determine ligand binding

To assess the feasibility of using nuclear Overhauser effect (NOE) based NMR experiments to detect binding between FabF and ligands, saturation transfer difference (STD) spectra were obtained for platensimycin and platencin in the presence of *Pa*FabF C164A in a 10:1 ratio. Attenuation of the compound signals was observed for platencin (Figure 5), but not for the stronger binding platensimycin (Figure S4). The absence of signals for platensimycin is probably due to its slow off-rate causing the high binding affinity (0.52 μM) and resulting in a too slow exchange between free and bound ligand to be detectable.[38] Nevertheless, the data demonstrates that STD NMR measurements can be used to detect ligands binding with medium affinity to *Pa*FabF C164A.

ChemMedChem

Full Papers
doi.org/10.1002/cmdc.202100302

Chemistry Europe
European Chemical
Societies Publishing

Figure 5. Stacked STD NMR spectra displaying the signals from the aromatic and enone protons. Off-resonance (black), difference spectrum scaled ×4 (red) and difference spectrum for ligand in pure buffer (blue) obtained with platencin in a 10:1 ratio with *Pa*FabF C164A.

Robust soaking conditions for *Pa*FabF

Starting from our previously established crystallization conditions for *Pa*FabF C164Q,[34] the experimental setup was optimized to allow for reliable and highly repeatable crystallization of the protein. This included testing of different protein and precipitant concentrations, drop-to-buffer ratios, and freeze/thaw cycles. Under the optimized conditions, crystals were obtained in ~2/3 of all drops set up in 96 well plates. Moreover, the maximum DMSO concentration that the crystals could tolerate was determined and different soaking times were tested to establish conditions that would allow for a large number of well-diffracting crystals after soaking. Finally, crystal handling and fishing were improved. Since *Pa*FabF C164Q crystalized as stacked plates originating from the same centre (Figure S2), fishing as few plates as possible was very important for high quality diffraction and data processing. As a proof of concept, *Pa*FabF C164Q was soaked with platensimycin and the structure of the complex was determined at a resolution of 1.80 Å (Table S1, Figure S1). As expected, the ligand adopted the same binding mode as observed before for *Ec*FabF C163Q (Figure S1a). Compared to the apo structure, Phe400 was rotated to create space to bind the ligands (Figure S1b), as was also observed earlier for *Ec*FabF (Figure 3).

### The experimental toolbox put into action

Having established binding assays for *Pa*FabF and robust soaking conditions, the suitability of the experimental toolbox to support structure-based design of FabF inhibitors was subsequently evaluated. To this end, a virtual screen for FabF inhibitors was conducted, and binding of the shortlisted compounds was determined using the assays of the toolbox.

Virtual screening for FabF ligands binding into the malonyl pocket

For virtual screening, the malonyl binding site of FabF was targeted, as most known inhibitors bind into this pocket. As a first step, the binding sites of FabF orthologs were analysed. Alignment of the available crystal structures in the Protein Data Bank (PDB) revealed a rigid binding site with only Phe400 adopting two different rotamers (Figure 3). As mentioned above, in the apo wild type structure, Phe400 blocks the malonyl binding site while upon binding of a fatty acid or inhibitors like cerulenin or platensimycin it rotates into the open conformation. The open conformation is also present in the *Pa*FabF C164Q variant mimicking the acyl-enzyme intermediate (PDB ID: 4JB6) which was therefore used as template for virtual screening.

A pharmacophore hypothesis for malonyl binding site ligands was generated based on the binding modes of known inhibitors. Several structures of FabF in complex with platensimycin or derivatives thereof, cerulenin and a fatty acid were available in the public domain. To increase the diversity of the ligands, the structure of thiolactomycin in complex with the homologous protein FabB was also taken into account. Analysis of these structures suggested that hydrogen-bond interactions to His304 and His341 are crucial for binding as these were formed by all ligands studied. Thus, these interactions were included as mandatory in a pharmacophore model (Figure 6). Further, the backbone amide of Thr271 and the side chain hydroxyl group of Thr308 were found to form hydrogen bonds with platensimycin and its derivatives, and Phe400 to form edge-to-face interactions with the phenyl rings of these ligands (Figure 3). These interactions were included as optional features in the pharmacophore hypothesis but only two of them had to be fulfilled to satisfy the pharmacophore requirements.

A hierarchical approach was adopted for virtual screening. First, an updated version of our in-house prepared database of
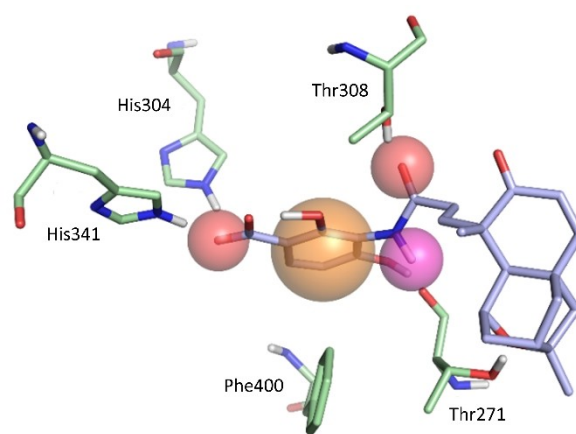
Figure 6. Pharmacophore model for FabF inhibitors binding into the malonyl- pocket. The interactions with the His residues were set to mandatory. In addition, two of the interactions to the Thr and Phe residues was required.
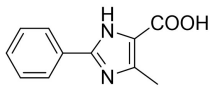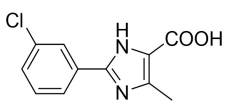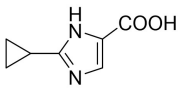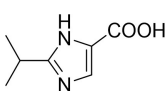
ChemMedChem

Full Papers
doi.org/10.1002/cmdc.202100302

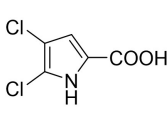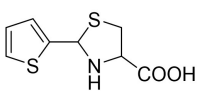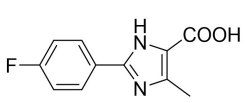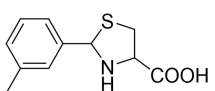**Chemistry Europe**
European Chemical
Societies Publishing

around 5 million commercially available compounds[39] was filtered for lead-like molecules fulfilling the above described pharmacophore. The resulting 66053 compounds were subsequently docked into the FabF binding site leading to binding modes for 48064 compounds. Filtering the rigid binding poses again with the pharmacophore resulted in 13244 compounds. Those were ranked by their calculated ligand efficiencies,[40] and the 1000 highest-ranked poses were inspected by eye (the predicted binding modes are available as Supporting Information). The poses were rated based on the quality of the putative hydrogen bonds and the ligand conformations. Fragment-sized ligands forming the desired hydrogen bonds to His304 and His341 were prioritized for purchase. As these interactions were formed well by carboxylic groups as also observed for platensimycin (Figure 3), all short-listed compounds contained this functionality. Finally, 8 compounds, all of them fragment-sized, were selected for hit validation (Table 1).
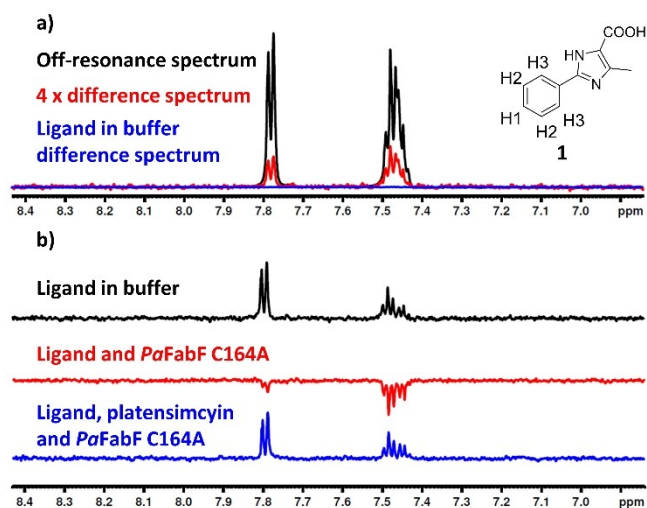
Testing of virtual screening hits

The 8 purchased virtual screening hits were tested as singletons at a concentration of 500 μM with STD and WaterLOGSY NMR in the presence of PaFabF C164A. For compounds **6** and **8** some attenuation of the WaterLOGSY signal was observed for ligand in pure buffer indicating compound aggregation (Figures S6d and f). All compounds showed binding in STD NMR experiments (Figure 7a and Figure S5). As an indication of binding strength, the STD_{ratio} for all compounds was calculated by dividing the integral of the most attenuated peak in the aromatic region of the difference spectra by the corresponding integral in the off spectra (Table 1). It was recently shown that the STD_{ratio} is roughly inversely proportional to K_D.[41] While the ratio is influenced by the extent of NOE magnetisation transfer from protein to ligand, dissociation rate and effective ligand concentration, these influences should be minimized across variable fragment scaffolds by only considering the strongest

Table 1. Compounds shortlisted for testing with PaFabF C164A after virtual screening together with binding data. STD_{ratio} was calculated by dividing the integral of the most attenuated peak in the aromatic region of the difference spectra by the corresponding integral in the off spectra. ✓ indicates that binding and x that no binding was observed in WaterLOGSY. % displacement indicates the extent to which platensimycin displaces the fragment from the binding site in WaterLOGSY competition experiments.

#	Structure	STD_{ratio} ($\times 10^{-3}$)	WaterLOGSY	Displacement [%]
1		65	✓	95
2		192	✓	74
3		9	x	
4		6	x	
5		240	✓	31
6		59	✓	ND[a]
7		77	✓	88
8		89	✓	ND[a]

[a] Could not be determined due to compound aggregation.

ChemMedChem

Full Papers
doi.org/10.1002/cmdc.202100302

**Chemistry
Europe**

European Chemical
Societies Publishing

Figure 7. Example from NMR binding assays with a virtual screening hit. a) Overlayed spectra of **1** from STD experiments. b) Stacked WaterLOGSY spectra. Binding of **1** can be outcompeted with platensimycin.

STD signal in the aromatic region and using presumably weakly binding, fast exchanging ligands. Six compounds (**1**, **2**, and **5**–**8**, Table 1) also showed binding in WaterLOGSY experiments and were progressed to competition experiments (Figure 7b, Figure S6). For all of them, binding to *Pa*FabF C164A (at a fragment concentration of 400 μM) could be at least to some extend outcompeted by addition of platensimycin at a final concentration of 10 μM (Figure 7b, Figure S5). This indicates that these compounds bind like platensimycin into the malonyl binding site as intended in the virtual screening. Under the assumption that the compounds bind at the tested concentration specifically into this pocket, the extent of fragment displacement by platensimycin was quantified in % by the ratio between a selected peak integral in the competition spectra and the corresponding integral in the reference spectra (Table 1). This means that the higher the % displacement, the weaker the fragment binds into the malonyl binding site. For **6** and **8**, the binding was not quantified due to compound aggregation in buffer reference spectra. For the remaining compounds, the affinity ranking based on platensimycin competition agreed with the ranking based on STD_{ratio} with **5** being the most potent ligand among the hits.

All compounds that showed binding in the NMR experiments were advanced to BLI experiments. The compounds were tested at concentrations ranging from 16 μM to 2 mM. At lower concentrations no binding and at higher concentrations ($\geq$ 500 μM for **6** and **8**, $\geq$ 1 mM for the remaining compounds) binding to both protein-loaded and biocytin-blocked reference sensors was observed, prohibiting the determination of binding constants (data not shown).

Next, we attempted to determine the binding modes of the compounds, and this was successful for one of the hits (Figure 8). The structure was obtained with re-synthesised material of **6** (compound **6 a** in Table 2) as we did not have enough of the purchased material left over from the binding

studies. The purchased material was a mixture of all four possible stereoisomers. However, in the virtual screen, only the (4*R*)-isomers scored well. Therefore, this stereocenter was fixed during synthesis while for the other stereocenter both configurations were obtained (Scheme 1). The structure of the complex *Pa*FabF C164Q-**6 a** was determined at 1.78 Å resolution (Table S1) with the ligand clearly visible in the difference electron density map (Figure 8a). Based on the electron density it was not possible to assign the stereochemistry of the compound as density around the undefined stereo centre was lacking. However, it appeared that the (2*S*,4*R*) diastereomer showed a better fit with the density than the (2*R*,4*R*) diastereomer (Figure S3a) and thus, only this ligand was modelled in the final structure. In the determined binding mode, the ligand forms hydrogen bonds to the catalytic histidines and the backbone of Phe399 (Figure 8b). While the interactions with the histidines are close to those predicted by docking, the thiazolidine moiety is clearly placed in a different position (Figure 8c). Accordingly, the bound ligand does not fulfil the postulated pharmacophore hypothesis.
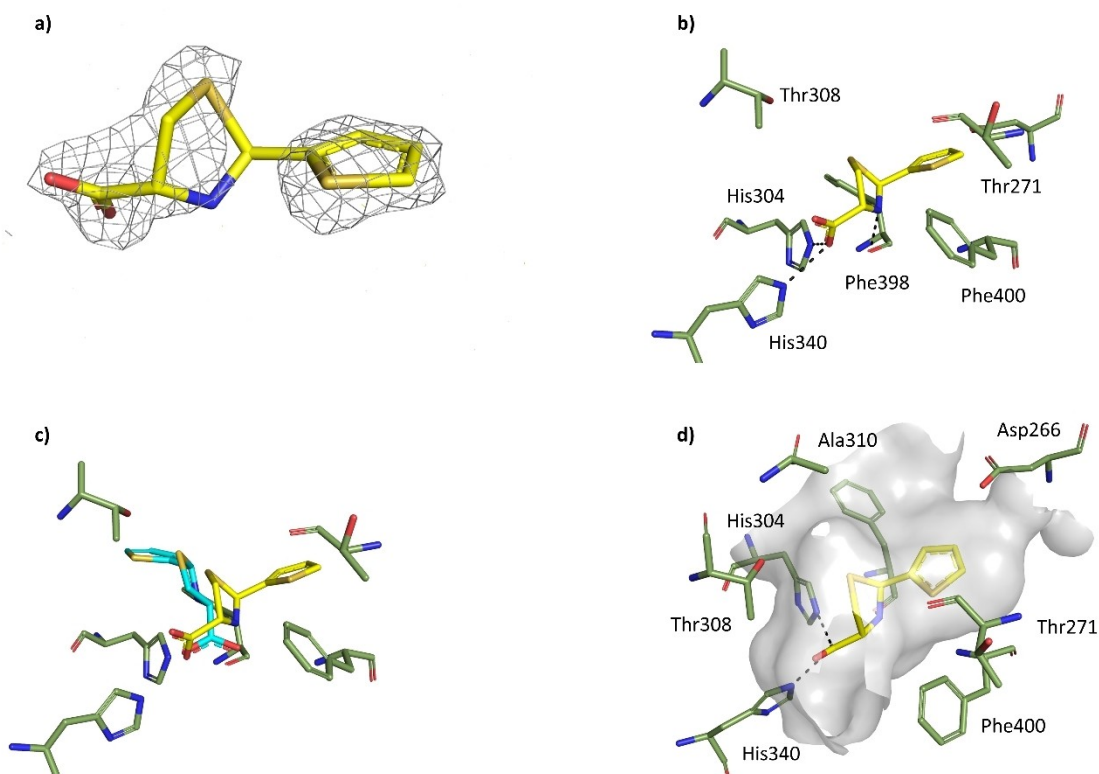
Different protein variants were used for obtaining binding data and crystal structures. This was done because the C164A variant behaved well in the binding assay while the C164Q variant led to well diffracting crystals and the affinities of platensimycin for both variants were comparable. For *Ec*FabF, complex structures with platensimycin were determined using both variants resulting in identical binding modes.[13,19] As the carboxylic groups of platensimycin and **6 a** superimpose well in the structures determined with *Pa*FabF C164Q and both ligands form comparable interactions in this part of the binding pocket (Figure S3b) it is likely that **6 a** like platensimycin adopts the same binding mode in both variants.

Hit expansion

Two thiazolidines were among the screening hits (**6** and **8**, Table 1), and for one of them the binding mode could be determined (Figure 8). Therefore, we chose this compound class for hit expansion. First, the hits were resynthesized to establish the synthesis and deliver more material for testing (**6 a** and **f**, Table 2). As docking had suggested that only the (4*R*) enantiomer could bind, this centre was fixed. In an effort to increase the affinities and solubilities of the compounds, analogues were designed. In particular, compounds **6 b** and **c** were meant to better fill the space in the area in which the thiophene ring of **6 a** was placed, compounds **6 g** and **h** to form additional hydrogen bonds with Asp266, and compound **6 d** to increase solubility (Figure 8d and Table 2). As the building block
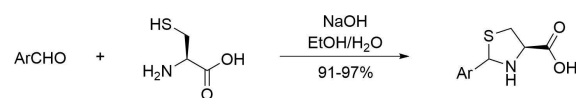
Scheme 1. Synthesis of substituted thiazolidines through a cyclodehydration reaction between L-cysteine and aryl aldehydes.

ChemMedChem

Full Papers
doi.org/10.1002/cmdc.202100302

Chemistry
Europe
European Chemical
Societies Publishing

Figure 8. Binding of compound **6a** to PaFabF C164Q (PDB ID 7OC0). a) Fo-Fc map of **6a** binding to PaFabF C164Q, contoured at 3.0 sigma. b) Interactions between **6a** (yellow) and PaFabF C164Q (green). Hydrogen-bonds are indicated as dashed lines. c) Alignment between the docked pose (cyan sticks) and the crystallographically determined binding mode of **6a** (yellow sticks). d) Solvent accessible surface of the PaFabF C164Q binding site indicating available space around the thiophen group of the ligand and the possibility to grow the compounds to form additional interactions with the close by Asp266.

for **6e** was available in the lab, this compound was synthesised as well.
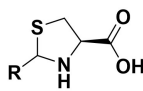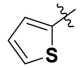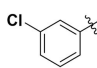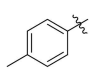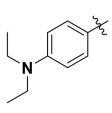
A general methodology for condensation of L-cysteine hydrochloride with aromatic aldehydes in presence of sodium hydroxide in ethanol gave the desired thiazolidines **6a**–**h** (Scheme 1, Table 2). In addition to providing diastereomers of hit molecules **6a** and **6f** with a fixed R-configuration at C-4, six more analogues of the hits were synthesized. The compounds were obtained in 91–97% yields. The synthesis yielded a mixture of diastereomers where aldehydes with electron-rich rings favoured formation of the (2S,4R) isomer over the (2R,4R) isomer (10:1 ratio for **6d**, Table 2) based on comparison of chemical shifts with those published for similar structures.[42] In most of the cases the diastereomeric ratio was found to be between 1:1 to 4:1. Separation of the individual diastereomers was not carried out at this stage and all compounds were tested as mixtures.

The analogues were tested for binding to PaFabF C164A using binding assays and PaFabF C164Q using X-ray crystallography. Two of the compounds were not soluble under the as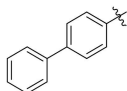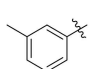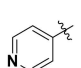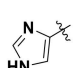say conditions (**6d** and **e**) and **6h** decomposed during shipping, thus, these were not further considered. For the remaining compounds, some attenuation of the WaterLOGSY signal was already observed for ligand in pure buffer indicating compound aggregation (Figure 9 and Figure S7). All tested compounds showed binding to PaFabF C164A at 1 mM using WaterLOGSY
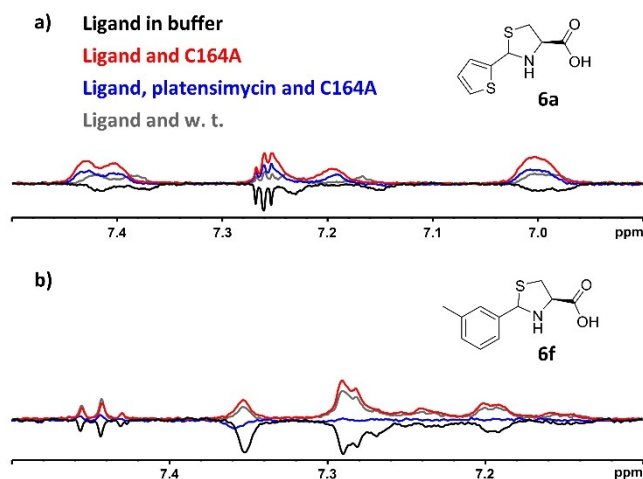
Figure 9. Overlay of WaterLOGSY spectra showing ligand in pure buffer (black), ligand with PaFabF C164A (red), ligand with PaFabF C164A and platensimycin (blue) and ligand with w.t. PaFabF (gray). a) Compound **6a** showed a stronger signal) with only PaFabF C164A than in competition and w.t. experiments. b) Compound **6f** showed a similar signal with PaFabF C164A and the w.t. enzyme while the signal in the competition experiment was weaker.

ChemMedChem

Full Papers
doi.org/10.1002/cmdc.202100302

Chemistry Europe
European Chemical
Societies Publishing

Table 2. Analogues of virtual [RB1] screening hit **6**. All compounds were assessed for binding to *Pa*FabF C164A. Competition experiments were carried out with platensimycin as competing ligand. ✓ indicates binding (C164A) or out-competing of binding with platensimycin (Competition). For WaterLOGSY no w.t., ✓ indicates that the signals for the competition experiment were similar to the signals with w.t. enzyme (low binding to the w.t. enzyme), while x indicates no difference in the signal for w.t. enzyme and *Pa*FabF C164A (binding to both enzymes).

#	Structure	Diastereomer ratio	WaterLOGSY		
6			C164A	Competition	no w.t.
a		3:2	✓	✓	✓
b		3:2	✓	_[a]	_[a]
c		1:1	✓	✓	✓
d		10:1	_[b]		
e		3:2	_[b]		
f		1.2:1	✓	✓	x
g		4:1	✓	✓	x
h		3:2	_[c]		

[a] Inconclusive experiment. [b] Compound was not soluble at 20 mM in DMSO. [c] Compound decomposed during shipment.

NMR (Table 2). However, competition experiments did not lead to a full reduction in WaterLOGSY signal. Considering that the compounds showed aggregation, this suggested that some of the WaterLOGSY signal stemmed from non-active site inter-actions. To further elucidate the binding mode of these compounds, experiments with w.t. *Pa*FabF were also carried out. For acidic compounds binding close to the catalytic histidines, one would expect no binding to the w.t. enzyme due to repulsion caused by the cysteine as observed for platencin and platensimycin. For compounds **6a** and **c**, binding to w.t. *Pa*FabF was reduced compared to *Pa*FabF C164A while for compounds **6f** and **g** the binding levels for both enzyme variants were comparable (Figure 9 and Figure S7). This could suggest that the compounds **6b** and **c** adopt a similar binding mode as **6a** closely interacting with the catalytic histidines while **6f** and **g** still bind into the malonyl binding site as their binding competes with platensimycin, however in a different orientation that is not affected by the presence or absence of the Cys164 side chain. Binding of **6b** was inconclusive, as some

signals were more intense in presence than in the absence of the competing ligand without a clear explanation (Figure S7b).

For none of the synthesised ligands, binding constants could be determined using BLI with either *Pa*AviFabF C164A or chemically biotinylated *Pa*FabF C164Q. Like the parent compounds, all compounds showed unspecific binding to the reference sensors at the highest concentrations (≥ 500 μM), and affinity was not improved to be in the measurable range by BLI. Likewise, determination of binding modes with soaking experiments was unsuccessful. In light of these results, the goal of synthesizing more potent and soluble analogues was not achieved.

Conclusion

FabF is an attractive target for antibiotics that was shown to be essential in several genetic screens.[7–11] Ligands with diverse scaffolds are needed to explore this target. Here, we have

ChemMedChem

Full Papers
doi.org/10.1002/cmdc.202100302

**Chemistry
Europe**
European Chemical
Societies Publishing

established an experimental toolbox to support structure-based drug discovery efforts for *Pa*FabF. We went on to use this toolbox to validate hits obtained from virtual screening.

The BLI assay allows for the determination of binding affinities. We have demonstrated that for the strong and medium affinity inhibitors platensimycin and platencin binding constants can be determined that are close to literature values (Figure 4). In principle, this method can also be used to determine binding of weaker ligands, however, this requires that the compounds are soluble at high enough concentrations.[43] The presumably mM binding constants and the propensity to form aggregates at these concentrations make the virtual screening hits and the synthesised analogues unsuited for BLI experiments. In most studies aiming at deriving SAR for platensimycin analogues no affinity or inhibition data was published. This is probably due to the complexity of inhibition, and binding assays used so far requiring either coupling enzymes in addition to other helper enzymes to synthesize the substrates and get a read-out or radiolabelled ligands.[13,44] In this respect, the BLI assay is nevertheless an important improvement making the determination of binding constants for FabF in principle straightforward.

The NMR assays we have set up are well suited to detect binding of ligands with medium to low affinity. In combination with a competing ligand or the use of different enzyme variants they can also deliver information about the binding sites of the compounds. In addition, STD$_{ratio}$[41] and % displacement can be used to rank compounds by affinity. In the case of the compounds were both values could be determined (**1**, **2**, **5** and **7**) they showed the same trends indicating that these measures are in agreement (Table 1).

Further, we have successfully optimized our previous crystallization conditions for *Pa*FabF C164Q to allow for soaking of small molecules in DMSO containing solutions.[34] We routinely obtain crystals diffracting to 1.7 Å allowing for detailed binding information for ligands. Nevertheless, for only one of the virtual screening hits a complex structure could be obtained. The frustratingly low rate of obtaining structural information for fragment hits has been reported before.[45] The reasons for this are not entirely clear, but it is possible that the binding affinity of the fragment hits in the assay buffer is different from the affinity in the soaking buffer causing the low success rate.

Virtual screening delivered 6 hits for which binding was confirmed using STD and WaterLOGSY experiments. However, the exact affinity could not be determined using BLI due to a combination of low solubility and low affinity. This is a common problem for fragment-sized compounds and some rounds of optimization based on structural information might be needed to obtain measurable affinity as also seen for other targets.[46] We have prioritized the compound for which we could determine the binding mode for optimization, as such information can dramatically improve the success rate.[47] Nevertheless, our attempts to optimize one of the compound has failed. Further efforts should be directed toward increasing the solubility of the compound series and exploring different parts of the binding site. Alternatively, optimizing the virtual screen-

ing hits **1**, **2**, **5** and **7** which showed no signs of aggregation in the WaterLOGSY assay could be promising. Among them, **2** and **5** appeared to be the most potent ones according to NMR data (Table 2).

This work has laid the foundation to support structure-based design efforts for *Pa*FabF ligands. The assays are also suitable for experimental fragment screening using NMR, BLI or X-ray crystallography and such efforts are ongoing to explore this promising target further.

Experimental Section

Expression and purification of *Pa*FabF variants

All genes except of w.t. *Pa*FabF and *Pa*FabF C164Q were synthesized and cloned into pET-28a-TEV vectors by Genscript (New Jersey). The protein constructs for FabF containing an AviTag[35] for BLI experiments (here called *Pa*AviFabF) were designed as follows: N-terminal His6-tag, TEV cleavage site, Avi-tag, followed by linker residues (GS). All FabF variants were expressed as described earlier,[34] with only minor deviations. Rosetta (DE3) pLysS competent *E. coli* cells (Novagen) were heat-shock transformed with the plasmids (45 s, 315 K) and cultured in autoinduction medium (1L LB with 50 mL 20X NPS, 20 mL 50X 5052 and 1 mL MgSO$_4$) supplemented with chloramphenicol (1 mL 30 mg/mL) and kanamycin (1 mL 50 mg/mL) for 48 h at 293 K with shaking at 250 rpm. Cells were harvested by centrifugation (45 min, 5000 g, 277 K), and each pellet resuspended in 30 mL lysis buffer [50 mM Na$_2$HPO$_4$ pH 7.8, 300 mM NaCl, 20 mM imidazole, 10% (v/v) glycerol, half a tablet of protease-inhibitor EDTA-free cocktail (Roche) and 0.05 mg DNase I (Sigma Aldrich)] and lysed on ice by sonication. The protein was purified as described earlier, but with a slight variation in gel filtration buffer [50 mM Na$_2$HPO$_4$, 150 mM NaCl, pH = 7.6, 10% (v/v) glycerol]. A high level of protein purity was confirmed by SDS-PAGE (Mini-PROTEAN TGX Stain-Free Precast Gel; Bio-Rad) and the yield, typically in excess of 10 mg/L, determined using Nanodrop 2000 (ThermoFisher).

Expression and purification of GST-BirA

The GST-BirA (*E. coli* biotin ligase fused to glutathione-S-transferase) pGEX-6P-1 vector was a kind donation from Petra Hänzelmann (University of Würzburg). The vector was transformed into Rosetta (DE3)pLysS competent *E. coli* cells (Novagen) and GST-BirA was expressed and purified as described earlier.[36]

Enzymatic biotinylation of *Pa*AviFabF variants

*Pa*AviFabF variants were biotinylated in a similar manner as described earlier.[36] In short, a 1 mL mixture of 100 μM *Pa*AviFabF, 1 μM GST-BirA, 5 mM MgCl$_2$, 150 μM D-biotin and 2 mM ATP in 1× PBS was incubated at 303 K for 1 h shaking at 60 rpm. 3 μL of 50 mM D-biotin and 50 μL of 20 μM GST-BirA in 1×PBS were then added, before the mixture was allowed to shake for another 1 h. 0.1 mL of Glutathione Sepharose (50% slurry in 1×PBS; Cytiva) was added and the resulting suspension incubated on ice for 1 h. The mixture was then centrifuged (2.000×g, 2 min) and the supernatant was brought through a prewashed (2 mL 1×PBS at 2.000×g, 2 min, twice) Zeba Spin desalting column (7 k Molecular weight cut-off; ThermoFischer) to remove the cofactors and the flow-through collected.

ChemMedChem

Full Papers
doi.org/10.1002/cmdc.202100302

Chemistry Europe
European Chemical
Societies Publishing

Chemical biotinylation of *Pa*FabF variants

*Pa*FabF C164Q and w.t. were chemically biotinylated by adding a 1.5 molar equivalent of NHS-PEG$_4$-biotin (ThermoFischer) to a 2 mL mixture of 10 μM FabF in 1×PBS. After reacting at rt for 30 min, the free NHS-PEG$_4$-biotin was removed using a prewashed (2 mL 1× PBS at 2.000×g, 2 min, twice) Zeba Spin desalting column (7k molecular weight cut-off; ThermoFischer).

BLI measurements

BLI measurements were performed using an Octet RED96 instrument (FòrteBio) in polypropylene 96-well F-Bottom microplates (Greiner Bio-One) at a constant temperature of 298 K. Wells contained a total volume of 200 μL liquid. The biotinylated proteins at a concentration of 500 μg/mL in assay buffer [1×PBS, 0.0001% (v/v) TritonX100, 5 mM DTT, 5% (v/v) DMSO] were immobilized onto Super Streptavidin (SSA) biosensors (FòrteBio). The loading was carried out in a series of sequential steps. Typically, first an initial baseline step of 300 s was used, followed by immobilization of the protein for 900 s until a response of 12–13 nm was reached when using enzymatically biotinylated AviFabF and 7–8 nm when using chemically biotinylated FabF. Unoccupied streptavidin sites were then quenched with biocytin (10 μg/mL) for 120 s, followed by a final washing step of 60 s in the assay buffer. Binding of compounds to *Pa*AviFabF (both w.t. and C164A), and biocytin blocked reference sensors was measured in three steps: 30 s baseline, 60 s association and 30–60 s disassociation. The obtained curves were analysed using the FortéBio software. The curves were aligned to their baselines and double-referenced against buffer wells and biocytin reference sensors. Binding constants were obtained by using a steady state model fitted to the averaged response obtained between 50 and 55 s. The reported K_D values are averages of four independent measurements, using two different protein batches for platencin, but the same protein batch for platensimycin. All fragments were tested in concentrations reaching from 15.6 μM to 2 mM.

Binding measurements using NMR

All NMR spectra were acquired in 3 mm NMR tubes at 298 K using a Bruker AVANCE NEO 600 MHz spectrometer (Bruker BioSpin, Zürich, Switzerland) equipped with a SampleJet and a QCI-P CryoProbe. Initial STD (stddiffesgp.3) and WaterLOGSY (ephogsygpno.2) screening of commercial compounds was carried out as singletons containing a final concentration of 500 μM ligand, 2.5 μM *Pa*FabF C164A, and follow up WaterLOGSY experiments were carried out with 400 μM ligand, 10 μM platensimycin and 2.5 μM *Pa*FabF C164A. All samples were dissolved in PBS buffer (pH = 7.4) containing 10% D$_2$O and 2.5% DMSO-d$_6$. Synthesized compounds were screened at 1 mM with 10 μM *Pa*FabF C164A, w.t. *Pa*FabF and 20 μM platensimycin for competition experiments in a similar buffer to above, but with 5% DMSO-d$_6$. STD spectra of platensimycin and platensin measurements were obtained using 100 μM ligand and 10 μM hisFabF C164A with 5% DMSO-d$_6$. Buffer controls were recorded in all cases. D-glucose was used as negative control (Figure S5i and S6e).

STD spectra were acquired using an on-resonance irradiation at 0.7 ppm and off-resonance irradiation at −40 ppm. A saturation time of 1 s and relaxation delay of 2 s were used. The number of scans was 256. WaterLOGSY experiments were conducted using a saturation time of 1 s and a mixing time of 1.7 s. The number of scans was 512.

The STD$_{ratio}$ was calculated by dividing the integral of the most attenuated peak in the aromatic region of the difference spectra by the integral of the corresponding peak in the off spectra. % displacement was calculated by dividing selected peak integrals in the competition spectra by the corresponding integral in the reference spectra. For compound **1**, **2** and **7** the methyl singlets at ~2.4 ppm and for compound **5** the singlet at ~6.6 ppm were used.

X-ray crystallography

Purified *Pa*FabF C164Q (14.5–15.6 mg/mL) was mixed with well buffer (0.20–0.24 M ammonium formate and 26%–31.2% PEG3350) at 0.8:0.9 μL drop ratio and let to equilibrate over 60 μL of well buffer in a 96 well plate at 25 °C using the vapor diffusion, sitting drop technique. Crystals were observed as large plates growing from the same centre within 24 hours and crystals growth continued for up to 3 days. For soaking, 300 nL of platensimycin and **6a** in solutions (2 and 50 mM respectively in 20% DMSO, 0.20 mM ammonium formate and 26% PEG3350) were added in the crystal drop and let to equilibrate for a maximum of 2.5 hours. Crystals were then fished and frozen in liquid nitrogen. X-ray data were collected at 100 K at the Biomax beamline, MaxIV synchrotron radiation facility in Lund Sweden. Dimple[48] from the CCP4i2 suite[49] was used for molecular replacement using the PDB ID: 4JB6 as input model. Modelled structures were manually inspected and corrected using Coot[50] while Refmac5[51] was used for the refinement of the crystal structures. Data collection, processing and refinement statistics are listed in Table S1. The complex *Pa*FabF-platensimycin has obtained the PDB ID 7OC1 and the complex *Pa*FabF-**6a** the PDB ID 7OC0.

Virtual screening

Modelling tasks were carried out using the Molecular Operating Environment (MOE; Chemical Computing Group, Montreal, QC, Canada) if not stated otherwise. The apo *Pa*FabF C164Q structure (PDB ID 4JB6) was used as template for docking. However, the side chain of Glu164 was modelled as cysteine to obtain an open malonyl-competitive binding site with a native catalytic triad. Polar hydrogen atoms were added, their positions energy minimized, and partial charges were assigned based on AMBER force field parameters. All water molecules were deleted. The polar aromatic head group of platensimycin was used to define a sphere set for ligand placement. Grid-based excluded volume, van-der-Waals potential, electrostatic potential and solvent occlusion maps were calculated as described earlier.[52,53] The partial charges of His304 and His341 were adjusted to favour hydrogen bonds to these residues. For that purpose, the partial charge of NE2 was reduced by 0.3 and the partial charge of HNE was increased by 0.3, keeping the net charge constant. The setup was validated by predicting the binding mode of platensimycin which resulted in a pose with all key interactions preserved.

A pharmacophore for FabF inhibitors was derived from the binding modes of known binders (platensimycin and its derivatives, thiolactomycin and cerulenin). Also structures of the homologue protein FabB were taken into account to increase the diversity of ligands. The final pharmacophore setup contained an essential hydrogen bond acceptor feature to His304 and His341 and three optional features of which at least 2 needed to be fulfilled: a hydrogen-bond acceptor to Thr308, a hydrogen-bond donor to Thr271 and an aromatic feature for the interaction with Phe400 (Figure 6). The radii for all hydrogen-bond features were set to 1 Å and the radius for the hydrophobic interaction was set to 1.5 Å.

ChemMedChem

Full Papers
doi.org/10.1002/cmdc.202100302

**Chemistry
Europe**
European Chemical
Societies Publishing

Our in-house prepared MySQL database of around 5 million commercially available compounds from various suppliers was filtered for lead-like molecules fulfilling the following criteria: no unwanted groups, no ring systems with more than two fused rings, 10–30 heavy atoms, 1–7 hydrogen-bond acceptors, 1–3 hydrogen-bond donors, $-3 \leq$ clogP < 3, number of rotatable bonds < 8, number of nitril groups < 2, 1–3 ring systems.[39] The filtered compounds were protonated, tautomerized and stereoisomerized using in-house python scripts based on OpenEye's OEChem toolkit (OEChem, version 2016.6.1, OpenEye Scientific Software, Inc., Santa Fe, NM, USA) (scripts are available at https://github.com/ruthbrenk/compound_preparation). Conformers were generated using OpenEye's OMEGA toolkit. Subsequently, filtered and prepared molecules were screened with the above described pharmacophore. Compounds that passed the pharmacophore filter were transformed into a format suitable for docking as described previously.[54]

The prepared compounds were docked into the receptor using DOCK 3.6.[53,55,56] Docking parameters were set as follows: ligand and receptor bins 0.4 Å, overlap bins 0.2 Å and distance tolerance for matching ligand atoms to receptor matching sites 1.5 Å. For each compound, the best scored representative was stored in the docking hit list. Docking poses were analysed using MOE. First, rigid docking poses were filtered with the pharmacophore described above. Subsequently, the compounds passing this filter were ranked by their predicted ligand efficiency which was calculated as docking score/number of heavy atoms[40] and the 1000 highest-ranked poses were inspected by eye.

Design of analogues of compound 6

Compounds with substitutions in the 2-position of the thiazolidine ring were drawn in Maestro (Schrödinger Release 2018-1: Maestro, Schrödinger, LLC, New York, NY, 2021) and minimized in the *Pa*FabF C164Q binding site. Compounds that explored additional interactions in the pocket in which the thiophene ring was placed and/or that filled available space in the binding site adjacent to this ring (Figure 8d) were shortlisted for synthesis.

Chemical compounds

Platensimycin was purchased from Sigma Aldrich and platencin was purchased from Cayman Chemicals. The virtual screening hits **1**–**7** were purchased from Enamine Ltd., virtual screening hit **8** from Vitas-M Laboratory Ltd. Identities were confirmed using ^{1}H NMR and HRMS (see Supporting Information).

Synthesis

Synthesis of compounds **6a**–**h** (Table 2) is described in the Supporting Information.

Supporting Information

The Supporting Information includes an SD file containing predicted binding modes of the top 1000 compounds together with scores, number of heavy atoms and ligand efficiencies. There is also a file with additional Figures and synthetic methods.

Conflict of Interest

The authors declare no conflict of interest.

Keywords: antibiotics · bio-layer interferometry · ligand-based NMR · structure-based design · virtual screening

[1] E. D. Brown, G. D. Wright, *Nature* **2016**, *529*, 336–343.
[2] E. Tacconelli, E. Carrara, A. Savoldi, S. Harbarth, M. Mendelson, D. L. Monnet, C. Pulcini, G. Kahlmeter, J. Kluytmans, Y. Carmeli, M. Ouellette, K. Outterson, J. Patel, M. Cavaleri, E. M. Cox, C. R. Houchens, M. L. Grayson, P. Hansen, N. Singh, U. Theuretzbacher, N. Magrini, *Lancet Infect. Dis.* **2018**, *18*, 318–327.
[3] U. Theuretzbacher, K. Bush, S. Harbarth, M. Paul, J. H. Rex, E. Tacconelli, G. E. Thwaites, *Nat. Rev. Microbiol.* **2020**, *18*, 286–298.
[4] J. Yao, C. O. Rock, *Biochim. Biophys. Acta, Mol. Cell Biol. Lipids* **2017**, *1862*, 1300–1309.
[5] F. J. Asturias, J. Z. Chadick, I. K. Cheung, H. Stark, A. Witkowski, A. K. Joshi, S. Smith, *Nat. Struct. Mol. Biol.* **2005**, *12*, 225–232.
[6] A. J. Kastaniotis, K. J. Autio, J. M. Kerätär, G. Monteuuis, A. M. Mäkelä, R. R. Nair, L. P. Pietikäinen, A. Shvetsova, Z. Chen, J. K. Hiltunen, *Biochim. Biophys. Acta, Mol. Cell Biol. Lipids* **2017**, *1862*, 39–48.
[7] B. E. Poulsen, R. Yang, A. E. Clatworthy, T. White, S. J. Osmulski, L. Li, C. Penaranda, E. S. Lander, N. Shoresh, D. T. Hung, *Proc. Nat. Acad. Sci.* **2019**, *116*, 10072–10080.
[8] K. H. Turner, A. K. Wessel, G. C. Palmer, J. L. Murray, M. Whiteley, *Proc. Nat. Acad. Sci.* **2015**, *112*, 4110–4115.
[9] S. A. Lee, L. A. Gallagher, M. Thongdee, B. J. Staudinger, S. Lippman, P. K. Singh, C. Manoil, *Proc. Nat. Acad. Sci.* **2015**, *112*, 5189–5194.
[10] D. Skurnik, D. Roux, H. Aschard, V. Cattoir, D. Yoder-Himes, S. Lory, G. B. Pier, *PLoS Pathog.* **2013**, *9*, e1003582.
[11] N. T. Liberati, J. M. Urbach, S. Miyata, D. G. Lee, E. Drenkard, G. Wu, J. Villanueva, T. Wei, F. M. Ausubel, *Proc. Nat. Acad. Sci.* **2006**, *103*, 2833–2838.
[12] A. Sarkar, R. Brenk, *PLoS One* **2015**, *10*, e0137279.
[13] J. Wang, S. M. Soisson, K. Young, W. Shoop, S. Kodali, A. Galgoci, R. Painter, G. Parthasarathy, Y. S. Tang, R. Cummings, S. Ha, K. Dorso, M. Motyl, H. Jayasuriya, J. Ondeyka, K. Herath, C. Zhang, L. Hernandez, J. Allocco, A. Basilio, J. R. Tormo, O. Genilloud, F. Vicente, F. Pelaez, L. Colwell, S. H. Lee, B. Michael, T. Felcetto, C. Gill, L. L. Silver, J. D. Hermes, K. Bartizal, J. Barrett, D. Schmatz, J. W. Becker, D. Cully, S. B. Singh, *Nature* **2006**, *441*, 358–361.

[14] Z. Feng, D. Chakraborty, S. B. Dewell, B. V. Reddy, S. F. Brady, *J. Am. Chem. Soc.* **2012**, *134*, 2981–2987.

[15] J. Wang, S. Kodali, S. H. Lee, A. Galgoci, R. Painter, K. Dorso, F. Racine, M. Motyl, L. Hernandez, E. Tinney, S. L. Colletti, K. Herath, R. Cummings, O. Salazar, I. González, A. Basilio, F. Vicente, O. Genilloud, F. Pelaez, H. Jayasuriya, K. Young, D. F. Cully, S. B. Singh, *Proc. Nat. Acad. Sci.* **2007**, *104*, 7612–7616.

[16] S. Kauppinen, M. Siggaard-Andersen, P. von Wettstein-Knowles, *Carlsberg Res. Commun.* **1988**, *53*, 357–370.

[17] G. D'Agnolo, I. S. Rosenfeld, J. Awaya, S. Omura, P. R. Vagelos, *Biochim. Biophys. Acta* **1973**, *326*, 155–156.

[18] I. Nishida, A. Kawaguchi, M. Yamada, *J. Biochem.* **1986**, *99*, 1447–1454.

[19] S. B. Singh, J. G. Ondeyka, K. B. Herath, C. Zhang, H. Jayasuriya, D. L. Zink, G. Parthasarathy, J. W. Becker, J. Wang, S. M. Soisson, *Bioorg. Med. Chem. Lett.* **2009**, *19*, 4756–4759.

[20] A. C. Price, K.-H. Choi, R. J. Heath, Z. Li, S. W. White, C. O. Rock, *J. Biol. Chem.* **2001**, *276*, 6551–6559.

[21] M. Moche, G. Schneider, P. Edwards, K. Dehesh, Y. Lindqvist, *J. Biol. Chem.* **1999**, *274*, 6031–6034.

[22] K. Tiefenbacher, J. Mulzer, *J. Org. Chem.* **2009**, *74*, 2937–2941.

[23] K. C. Nicolaou, G. S. Tria, D. J. Edmonds, *Angew. Chem.* **2008**, *120*, 1804–1807; *Angew. Chem. Int. Ed.* **2008**, *47*, 1780–1783.

[24] K. C. Nicolaou, A. Li, D. J. Edmonds, *Angew. Chem. Int. Ed.* **2006**, *45*, 7086–7090; *Angew. Chem.* **2006**, *118*, 7244–7248.

[25] A. K. Ghosh, K. Xi, *J. Org. Chem.* **2009**, *74*, 1163–1170.

[26] K. Tian, Y. Deng, L. Qiu, X. Zhu, B. Shen, Y. Duan, Y. Huang, *ChemistrySelect* **2018**, *3*, 12625–12629.

[27] K. C. Nicolaou, A. F. Stepan, T. Lister, A. Li, A. Montero, G. S. Tria, C. I. Turner, Y. Tang, J. Wang, R. M. Denton, D. J. Edmonds, *J. Am. Chem. Soc.* **2008**, *130*, 13110–13119.

[28] K. C. Nicolaou, T. Lister, R. M. Denton, A. Montero, D. J. Edmonds, *Angew. Chem.* **2007**, *119*, 4796–4798; *Angew. Chem. Int. Ed.* **2007**, *46*, 4712–4714.

[29] J. Wang, V. Lee, H. O. Sintim, *Chem. Eur. J.* **2009**, *15*, 2747–2750.

[30] J. Krauss, V. Knorr, V. Manhardt, S. Scheffels, F. Bracher, *Arch. Pharm.* **2008**, *341*, 386–392.

[31] M. Fisher, R. Basak, A. P. Kalverda, C. W. G. Fishwick, W. B. Turnbull, A. Nelson, *Org. Biomol. Chem.* **2013**, *12*, 486–494.

[32] Y. Deng, X. Weng, Y. Li, M. Su, Z. Wen, X. Ji, N. Ren, B. Shen, Y. Duan, Y. Huang, *J. Med. Chem.* **2019**, *62*, 6682–6693.

[33] Z. Zheng, J. B. Parsons, R. Tangallapally, W. Zhang, C. O. Rock, R. E. Lee, *Bioorg. Med. Chem. Lett.* **2014**, *24*, 2585–2588.

[34] B. Baum, L. S. M. Lecker, M. Zoltner, E. Jaenicke, R. Schnell, W. N. Hunter, R. Brenk, *Acta Crystallogr., Sect. F: Struct. Biol. Commun.* **2015**, *71*, 1020–6.

[35] D. Beckett, E. Kovaleva, P. J. Schatz, *Protein Sci.* **1999**, *8*, 921–929.

[36] M. Fairhead, M. Howarth, *Methods Mol. Biol.* **2015**, *1266*, 171–184.

[37] E. Martin, J. Wang, I. Zaror, J. Yu, K. Yan, M. Doyle, P. Feucht, K. Shoemaker, B. Warne, M. Chin, B. Sy, L. Leder, M. Meyerhofer, C.

[38] Wartchow, D. Yao, in *Label-Free Technol. Drug Discov.* (Eds.: M. Cooper, L. M. Mayr), John Wiley & Sons, Ltd, **2011**, pp. 223–240.

[38] J. Angulo, P. M. Nieto, *Eur. Biophys. J.* **2011**, *40*, 1357–1369.

[39] R. Brenk, A. Schipani, D. James, A. Krasowski, I. H. Gilbert, J. Frearson, P. G. Wyatt, *ChemMedChem* **2008**, *3*, 435–444.

[40] A. L. Hopkins, C. R. Groom, A. Alex, *Drug Discovery Today* **2004**, *9*, 430–431.

[41] A. L. Kantsadi, E. Cattermole, M.-T. Matsoukas, G. A. Spyroulias, I. Vakonakis, *J. Biomol. NMR* **2021**, *75*, 167–178.

[42] A. Y. Ershov, D. G. Nasledov, I. V. Lagoda, V. V. Shamanin, *Chem. Heterocycl. Compd.* **2014**, *50*, 1032–1038.

[43] C. A. Wartchow, F. Podlaski, S. Li, K. Rowan, X. Zhang, D. Mark, K.-S. Huang, *J. Comput.-Aided Mol. Des.* **2011**, *25*, 669.

[44] J. G. Borgaro, A. Chang, C. A. Machutta, X. Zhang, P. J. Tonge, *Biochemistry* **2011**, *50*, 10678–10686.

[45] E. Hassaan, P.-O. Eriksson, S. Geschwindner, A. Heine, G. Klebe, *ChemMedChem* **2020**, *15*, 324–337.

[46] A. C. Gibbs, M. C. Abad, X. Zhang, B. A. Tounge, F. A. Lewandowski, G. T. Struble, W. Sun, Z. Sui, L. C. Kuo, *J. Med. Chem.* **2010**, *53*, 7979–7991.

[47] P. J. Hajduk, J. Greer, *Nat. Rev. Drug Discovery* **2007**, *6*, 211–219.

[48] M. Wojdyr, R. Keegan, G. Winter, A. Ashton, *Acta Crystallogr. Sect. A* **2013**, *69*, s299.

[49] L. Potterton, J. Agirre, C. Ballard, K. Cowtan, E. Dodson, P. R. Evans, H. T. Jenkins, R. Keegan, E. Krissinel, K. Stevenson, A. Lebedev, S. J. McNicholas, R. A. Nicholls, M. Noble, N. S. Pannu, C. Roth, G. Sheldrick, P. Skubak, J. Turkenburg, V. Uski, F. von Delft, D. Waterman, K. Wilson, M. Winn, M. Wojdyr, *Acta Crystallogr., Sect. D: Struct. Biol.* **2018**, *74*, 68–84.

[50] P. Emsley, K. Cowtan, *Acta Crystallogr., Sect. D: Struct. Biol.* **2004**, *60*, 2126–2132.

[51] G. N. Murshudov, P. Skubák, A. A. Lebedev, N. S. Pannu, R. A. Steiner, R. A. Nicholls, M. D. Winn, F. Long, A. A. Vagin, *Acta Crystallogr., Sect. D: Biol. Crystallogr.* **2011**, *67*, 355–367.

[52] R. Brenk, J. J. Irwin, B. K. Shoichet, *J. Biomol. Screening* **2005**, *10*, 667–674.

[53] M. M. Mysinger, B. K. Shoichet, *J. Chem. Inf. Model.* **2010**, *50*, 1561–1573.

[54] C. P. Mpamhanga, D. Spinks, L. B. Tulloch, E. J. Shanks, D. A. Robinson, I. T. Collie, A. H. Fairlamb, P. G. Wyatt, J. A. Frearson, W. N. Hunter, I. H. Gilbert, R. Brenk, *J. Med. Chem.* **2009**, *52*, 4454–4465.

[55] D. M. Lorber, B. K. Shoichet, *Protein Sci.* **1998**, *7*, 938–50.

[56] B. Q. Wei, W. A. Baase, L. H. Weaver, B. W. Matthews, B. K. Shoichet, *J. Mol. Biol.* **2002**, *322*, 339–355.